

ARTICLE

# Investigation of Point Merge Utilization Worldwide Using Opensky Network Data

Henrik Hardell,<sup>1,2</sup> Tatiana Polishchuk,<sup>1</sup> and Lucie Smetanová<sup>\*,1</sup>

<sup>1</sup>Linköping University, Norrköping, Sweden

<sup>2</sup>Airspace Unit, Luftfartsverket (LFV), Norrköping, Sweden

\*Corresponding author: lucie.smetanova@liu.se

(Received: 23 July 2024; Revised: 25 November 2024 and 29 January 2025; Accepted: 7 February 2025; Published: 21 February 2025)

(Editor: Junzi Sun; Reviewers: Raúl Sáez, Enrico Spinielli, and Aymeric Trzmiel)

## Abstract

Point Merge (PM) arrival procedures are currently in use at 44 airports across 20 countries worldwide. These procedures come in various design variants, including overlapping, partially overlapping, or separated sequencing legs. The positioning of sequencing legs within or outside of the Terminal Maneuvering Area (TMA) and the geometry of the arrival flows to PM or merging points impact the associated trade-offs between the PM system capacity and efficiency. In our study, we analyze the utilization of PM procedures at several airports implementing PM, using open-access ADS-B-based data from the Opensky Network. To identify flights that adhere to the PM procedures, we propose a catchment algorithm. The accuracy of the algorithm depends on the quality and completeness of the data, the specific design of the algorithm, and the complexity of the PM procedures. Generally, a well-designed catchment algorithm can achieve high accuracy by considering factors such as aircraft positions, speeds, and adherence to sequencing instructions. Then, we quantify PM utilization using performance indicators specifically tailored for this purpose.

This paper builds upon previous research presented at the 11th OpenSky Symposium in 2023. We introduce an additional step to enhance the accuracy of the catchment algorithm and conduct a comprehensive sensitivity analysis of the catchment area size employed in the initial stage. We quantify the algorithm's accuracy by considering false-positive and false-negative filtered trajectories. Furthermore, we compare the results of our proposed approach with the PM identification tool available in the Traffic Library.

**Keywords:** Arrival procedures, Key Performance Indicators, Point Merge, TMA

**Abbreviations:** ATM: Air Traffic Management, CDOs: Continuous Descent Operations, EGLC: London City airport, EIDW: Dublin airport, ENBR: Bergen airport, ENGM: Oslo Gardermoen airport, JOAS: Journal of Open Aviation Science, KPIs: Key Performance Indicators, PM: Point Merge, RKSI: South Korea Seoul Incheon airport, SKBO: Bogotá El Dorado airport, TMA: Terminal Maneuvering Area, ULLI: St. Petersburg Pulkovo airport

## 1. Introduction

The Point Merge (PM) procedure was developed in 2006 by the EUROCONTROL Experimental Centre (EEC). PM is a technique which simplifies merging of the arrival traffic flows, providing better opportunities for environmentally-efficient descents, including Continuous Descent Operations (CDOs), as well as noise reduction [1, 2, 3]. Since the development of PM procedure, many airports worldwide adopted the procedures.

Since the introduction of Area Navigation (RNAV), EUROCONTROL is proposing new options for merging traffic in the TMA. RNAV is defined as: "a method of navigation which permits aircraft operation on any desired flight path within the coverage of the station-referenced navigation aids or within the limits of the capability of self-contained aids, or a combination of these" [4]. The RNAV system provides precise position fixes for aircraft at all times. This capability allows aircraft to depart from the rigid ground-based conventional routes and engage in point-to-point navigation using a predefined set of waypoints.

The PM, as well as trombone systems, are the alternative variants for navigating aircraft in the TMA towards runway using predefined trajectory paths with assigned shortcuts, which became possible after introduction of the RNAV approaches.

An example of a Point Merge system is illustrated in Figure 1. PM features a single point to merge for several arrival flows. This differs from the widely used vectoring technique where traffic merges in different points of a TMA preceding the final approach, under constant supervision and guidance of Air Traffic Controllers (ATCOs). Before merging, aircraft are flying along the "quasi arcs" (or sequencing legs of the PM) equidistant from the merge point, used for path stretching/delay absorption when necessary. The ATCO issues a single "direct to" instruction to each aircraft along the legs as soon as the required spacing with the preceding aircraft is obtained. Such a design increases controllability, reduces controllers workload, quantified in the number of instructions given to the pilots, and provides better opportunities for greener arrival descents [5, 6, 7].

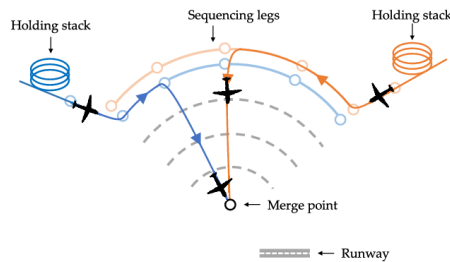


**Figure 1.** Point Merge System Visualization, source: [8]

There is a number of variants of the PM system implementation such as overlapping, partially overlapping, or separated sequencing legs. The positioning of PM system and different geometry of the flows to PM or merging to a point also differs among airports based on their design goals [9].

This paper extends our previous research [10] where we investigated how PM is utilized in different airports around the globe. We proposed an initial algorithm for identification of the arrival trajectories adherent to the PM procedures, and then quantified PM utilization applying the tailored metrics PM utilization and PM usage. In this paper, we introduce an additional step to enhance the accuracy of the catchment algorithm and conduct a comprehensive sensitivity analysis of the catchment area size employed in the initial stage. We quantify the algorithm's accuracy by considering false-positive and false-negative filtered trajectories. Furthermore, we compare the results of our proposed approach with the PM identification tool available in the Traffic Library. The purpose of this study is to understand to what extent the PM systems are utilized in different airports and to provide overview of the current usage of the procedures to the Air Traffic Control (ATC). The work is structured as follows: First, we present the overview of the related research in Section 2, then, in Section 3 we describe the airports chosen for this study, the data and the performance indicators. We present the catchment algorithm for identification of PM-adherent flights in Section 4. In Section 5 we discuss the PM usage and utilization for the chosen airports and finally, in Section 6 we conclude the findings and refer to future work.

## 2. Related Work

Several studies have examined the performance of Point Merge systems. In [11], the authors investigated early simulations of PM arrival procedures, with a specific focus on integrating PM into typical terminal airspace configurations. Additionally, an extensive study on the benefits and potential of PM was conducted in [3].

The authors of [12] proposed a novel PM design for Beijing Capital International airport and tested the resulting performance of the autonomous arrival management system. Later, the authors extended the work in [7] and introduced a Multi-layer Point Merge (ML-PM) system for autonomous arrival management. The authors also designed an efficient trajectory planning system for parallel runways with usage of the ML-PM route network.

The design and potential benefits of Point Merge systems have been explored in several thesis works. Researchers have investigated various aspects of PM, including system optimization, safety enhancements, and operational efficiency. The author of [13] proposed an innovative PM design specifically tailored for one of the runways at Amsterdam Schiphol Airport. The goal was to enhance the efficiency of arrival management by optimizing aircraft sequencing and spacing during approach. Another investigation took place at Palma de Mallorca Airport, reported in [14], with the focus on the potential of automatic scheduling of flights and design of an automated control tool.

The authors of [15] proposed a data-driven computer vision approach for the identification of PM structures in large datasets containing historical flight tracks. An alternative method for detecting PM structures was presented in [16], which involves analyzing geometrical pattern information in track data.

In [17], the authors analyzed arrival trajectories at five major European airports to assess inefficiencies associated with holding patterns, PM systems and CDOs. To identify trajectories adhering to PM systems at different airports, they utilized the method implemented in the Traffic library [18]. Several studies focused on the performance of PM systems under weather uncertainties, such as those detailed in [19].

Very recently, the authors in [20] suggested a novel approach as an extension to the PM structures with incorporated trombone-like double PM system to provide large delay absorption capacity in a small area.

In our previous work [21], we investigated the utilization of Point Merge systems at Oslo Gardermoen Airport and concluded that these systems are significantly underutilized. In this study, we enhance the PM catchment algorithm, generalizing it for application at airports worldwide, and evaluate PM performance using PM utilization and PM usage metrics.

## 3. Methodology

In this section, we present the methodology which we apply for identification and evaluation of the PM procedures. We describe the airports chosen for the studies, the data and the performance indicators used for PM evaluation.

### 3.1 Airports

According to Eurocontrol [22], PM is now operational for 44 airports in 20 countries and four continents. For our studies we've chosen the following seven airports: London-City airport (United Kingdom, Europe), Dublin (Ireland, Europe), Bergen (Norway, Europe), Oslo Gardermoen (Norway, Europe), Bogotá El Dorado (Colombia, South America), Seoul-Incheon airport (South Korea, Asia), and Pulkovo Airport St. Petersburg (Russia, Euro-Asia). Figure 2 shows example PM charts for each

of the chosen airports (note that the figure displays one example PM system per airport, not all the PM systems).

London City handled 49.000 movements in 2022 and operates with PM since 2016. The PM procedures consist of two overlapping arcs, used for both directions of the airport’s single runway.

Dublin is currently the only Irish airport operating with PM. The procedures were introduced in 2012 to its 10/28 runway, with fully overlapping legs to runway 28 and fully dissociated legs to runway 10. Since August 2022, the airport operates with a second parallel runway. In 2022 the airport facilitated 242.000 movements.

Bergen airport operates with PM to its single runway since 2014, and had 82.000 movements in 2022. There are two fully dissociated arcs for each runway direction.

Oslo-Gardermoen implemented PM in 2011 to both of its parallel runways, and it is the busiest airport in Norway, handling 163.000 movements in 2022. The PM procedures are of the overlapping type, where aircraft may be vertically separated on the arcs.

The first South American airport implementing PM (since 2017) is Bogotá El Dorado airport, which features three fully dissociated systems serving the two parallel runways. In 2022, the airport handled 297.000 movements.

Seoul Incheon airport in South Korea operates with PM since 2012. It handled 94.000 movements in 2022. The arrival procedures consists of a mix of PM and trombone structures.

The Russian airport of Pulkovo operates with four dissociated PM systems connected to its two parallel runways. At the airport, which handled 41.000 arrivals in 2022, PM is used since 2017.

**Table 1.** Investigated Airports

ICAO	Airport name	# of PM systems	Point Merge types	Runways	Movements 2022
EGLC	London City	One	Overlapping arcs	Single runway	49.000
EIDW	Dublin airport	Two	Both types	Two runways	242.000
ENBR	Bergen airport	Two	Dissociated arcs	Single runway	82.000
ENGM	Oslo Gardermoen	Four	Overlapping arcs	Two parallel	163.000
RKSI	Seoul Incheon	One	Overlapping arcs	Four runways	94.000
SKBO	Bogotá El Dorado	One	Overlapping arcs	Two runways	297.000
ULLI	St. Petersburg Pulkovo	Two	Overlapping arcs	Two parallel	41.000

### 3.2 Data

The historical flight data is provided by the Opensky Network [29]. The database contains geographical flight trajectory data in the form of state vectors at one-second resolution. The data is transmitted by the Automatic Dependent Surveillance Broadcast (ADS-B) aircraft transponders, and collected via sensors on the ground, supported by volunteers, industrial supporters, and academic or governmental organizations. Due to the non-reliable nature of the data transmission technology and collection technique, the raw data may be incomplete and sometimes contains erroneous records.

We apply multiple cleaning procedures to each dataset. First, we detect inconsistencies in the latitudes and longitudes and remove the fluctuations. Then, we apply Gaussian filter to smooth altitude fluctuations and remove all incomplete or damaged trajectories including outliers such as go-arounds, flights which do not land on the runway, flights with departure and arrival at the same airports (mostly helicopters), most non-commercial flights. Wherever needed, we divide the flight trajectories into smaller data subsets according to which runway they landed on. To achieve that,

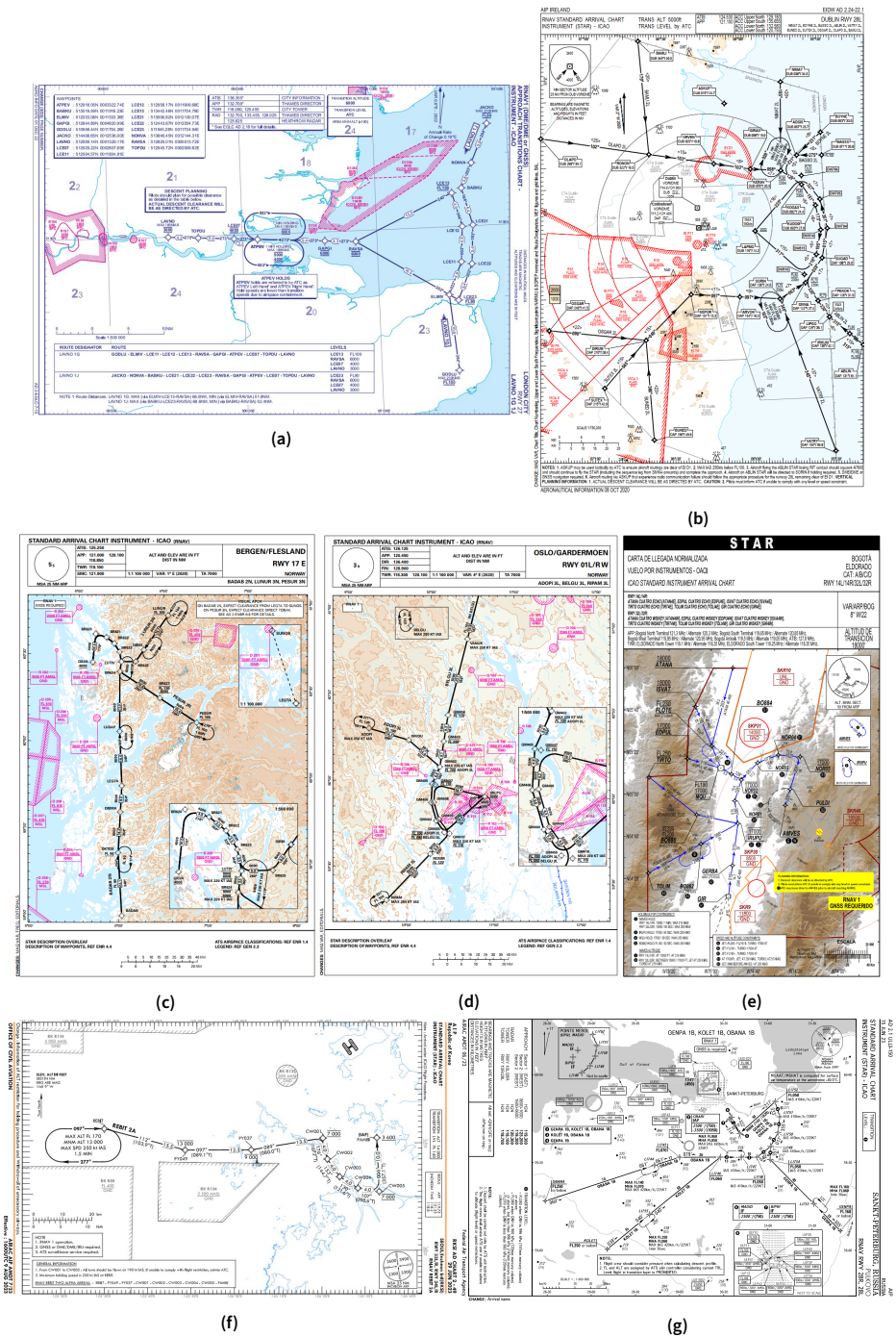


Figure 2. Example PM charts for the airports of London-City (a), Dublin (b), Bergen (c), Oslo-Gardermoen (d), Bogotá El Dorado (e), Seoul-Incheon (f) and St. Petersburg-Pulkovo (g). Sources: State AIPs of the respective countries [23] [24] [25] [26] [27] [28].

we detect the last 30 recordings of each flight, calculate the azimuth of the trajectory and assign the

flight to the corresponding runway based on the azimuth of the runway and heading of the flight in the last 30 seconds of the recording.

For each airport, we study one month of data for the year 2022, which was the year when the air traffic started to recover from the Covid-19 pandemic levels on most airports. We chose the busiest month of the year 2022 for each of the airports (see Table 2). The fifth column of the Table shows the number of aircraft trajectories in each data subset after the cleaning procedures. And the last column of the table corresponds to the percentage of the outlier flight trajectories removed from the initial dataset.

**Table 2.** Investigated Busiest Months in 2022

Airport ICAO	Country	City	Month	Arrivals (Opensky)	Outliers (%)
EGLC	United Kingdom	London City	June	2030 flights	0.2%
EIDW	Ireland	Dublin	July	8648 flights	1.2%
ENBR	Norway	Bergen	October	3464 flights	0.5%
ENGM	Norway	Oslo Gardermoen	October	7788 flights	0.2%
RKSI	South Korea	Seoul Incheon	December	1419 flights	19%
SKBO	Colombia	Bogotá El Dorado	December	8989 flights	5.1%
ULLI	Russia	St. Petersburg Pulkovo	August	6761 flights	0.6%

### 3.3 Performance Evaluation Metrics

In this subsection, we present the PM utilization and PM usage performance indicators. They were designed specifically for this kind of study and first described in [21].

#### 3.3.1 PM Usage

We define the **PM usage** by identifying the flights which adhere to the PM procedures, and calculating the proportion of these flights in the given dataset. This metric indicates the frequency of PM procedure usage during the period under consideration.

#### 3.3.2 PM Utilization

We define **PM Utilization** to evaluate what part of the PM sequencing legs is utilized by the flights. The PM Utilization metric indicates the proportion of the length of the PM sequencing leg flown by arriving aircraft compared to the full length of the corresponding PM sequencing leg, expressed as a percentage. To estimate this, we measure the distance along the sequencing leg from the starting point to the point when the aircraft was directed to turn towards the merge point and proceeded to the final approach. We apply small circles of  $\approx 3$  NM around each waypoint on the sequencing legs of each PM system to capture that (red and green circles in Figure 4). We chose the **PM Utilization** metric to capture the proportion of the arc utilized regardless the actual distance flown along the sequencing leg as the distances between the waypoints differ among airports, and also among different PM systems in the same airport.

## 4. Catchment Algorithm

In this section, we present the methodology developed for identification of the flight trajectories adhering to the PM procedures. The catchment algorithm is a two-step process, where on the first step we filter the flights based on their horizontal trajectories, visually check whether there are any falsely identified flights and, if so, the algorithm proceeds to the second step, in which we analyze the vertical profiles. The algorithm flow chart is shown in Figure 3.

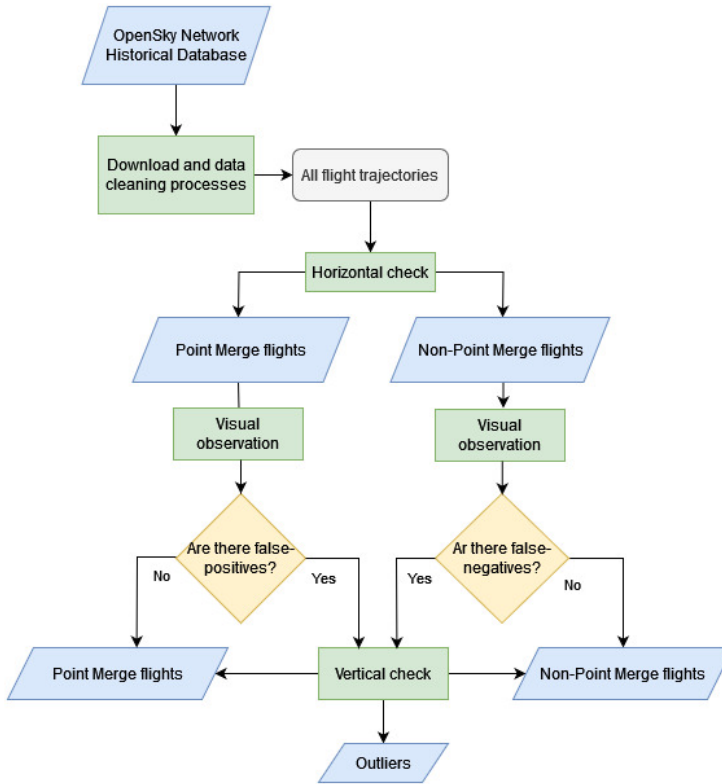


**Figure 3.** Flow chart of the catchment algorithm. Navigation: blue parallelograms represent the data subsets, green rectangles are processes, gray rectangle is the input data, and yellow squares represent conditional statements.

#### 4.0.1 Step 1: Horizontal Check

PM systems can have different configurations, and hence, the catchment algorithm which we use for identifying the flights adherent to the PM, has to be modified and fine-tuned for each airport individually. The idea is to consider a set of circular areas with the initial radius of about 3 NM around certain waypoints along the PM sequencing legs, and filter out all aircraft which did not pass through these areas. Figure 4 illustrates the technique applied to the North-Eastern part of the PM system at Oslo Gardermoen airport. The red and green circles representing the catchment areas are positioned around *GM418* and *GM423* waypoints which are the beginnings of PM legs. Colored curves in the figure illustrate the example flight trajectories performing PM procedure captured by the proposed technique.

Since the airports in our selection implemented various configurations of the PM systems, we have to position the catching area circles for each airport separately. Figures 5 - (a-h) illustrate the trajectories of the flights adherent to the chosen parts of the PM systems for each of the studied airports.

Arrival flights to **London City airport (EGLC)** often cross the PM system arcs, even when they don't perform the PM. Because of that, we detect the PM flights earlier before they enter the PM sequencing legs. This way we consider only the flights which passed both waypoints of the corresponding STARs: *NONVA* and *GODLU* waypoints marked with blue circles in Figure 5-(a) and the one at the start of the corresponding PM sequencing leg *BABKU* and *ELMIV* marked with red circles in Figure 5-(a).

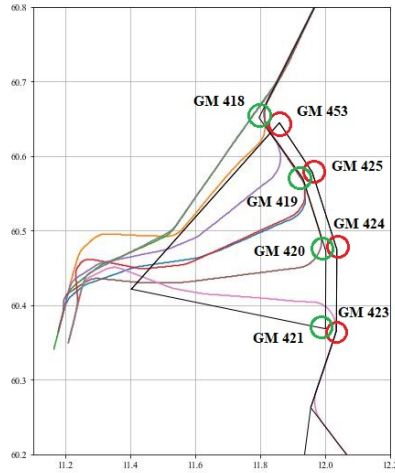


**Figure 4.** Example PM system at Oslo Gardermoen airport - North-Eastern part, with red and green circles around the waypoints along the sequencing legs, used for the calculation of the PM utilization KPI.

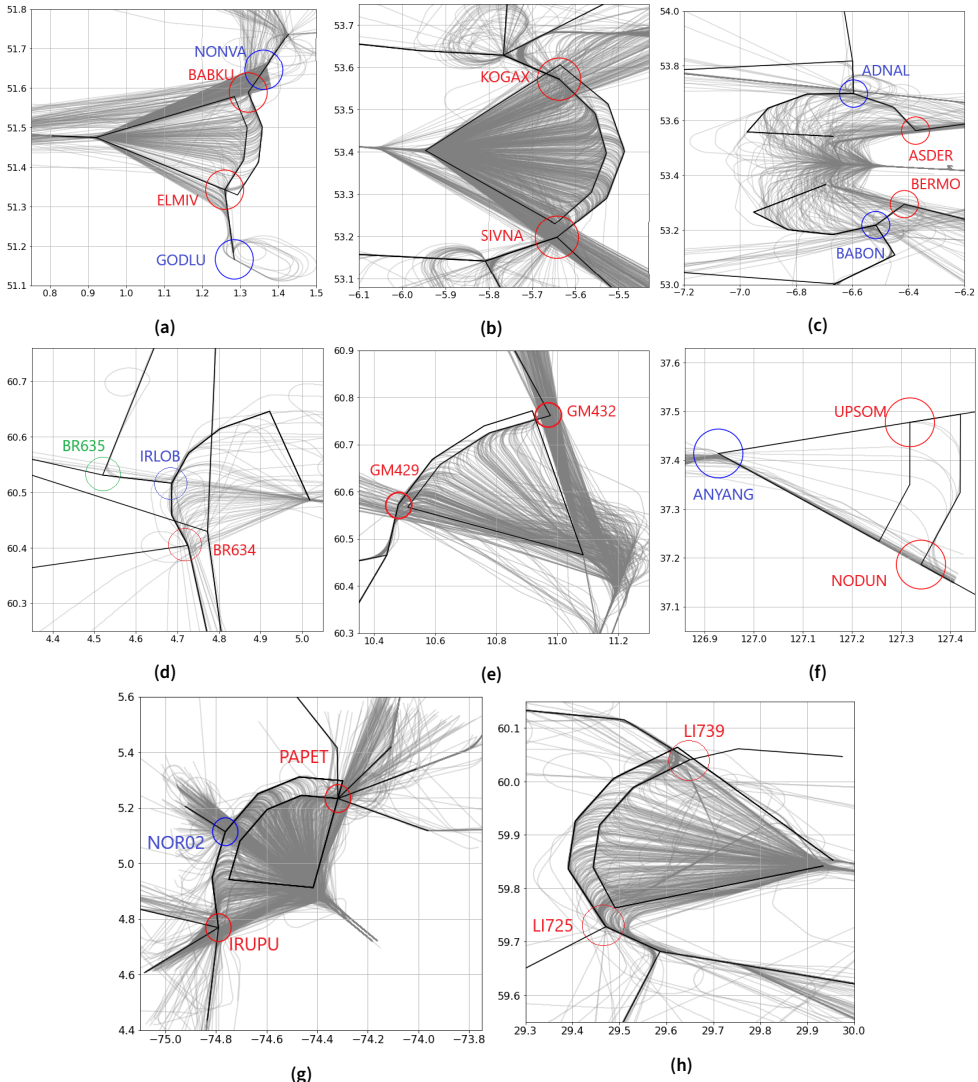
**Dublin airport (EIDW)** operates two different PM systems. We detect the flights performing the Eastern PM procedure by allocating catchment circle areas around the first waypoints *SIVNA* and *KOGAX* on the sequencing legs from each direction, marked with red circles (Figure 5 - b) . We apply the same technique to the Western PM systems, using the *ASDER* and *BERMO* waypoints, also marked with red circles. To account for the inbound traffic joining the arcs later, we also consider *BABON* and *ADNAL* waypoints, marked with blue circles (Figure 5 - c).

**Bergen airport (ENBR)** implemented two PM systems with fully dissociated sequencing legs. For each of the four PM parts, we position catchment circles around the first waypoint of the PM arc: *BR634*, *BR624*, *BR724*, *BR734* (marked with red color in Figure 5 - d), for NW, NE, SW, SE PM parts respectively. To catch only the flights performing PM and filter out the ones which just pass the waypoint on their way and then fly directly to the runway, we assign additional catchment areas around the earlier waypoints along the routes: *BR635* and *IRLOB* for NW, *BR625* and *LUTIV* for NE, *BR725* and *IBLIR* for SW, and *BR735* and *RATUG* for SE PM systems. *IRLOB*, *LUTIV*, *IBLIR*, and *RATUG* waypoints are marked with blue circles and the waypoints *BR635*, *BR625*, *BR725*, and *BR735* (marked with green circle in Figure 5 - d).

In **Oslo Gardermoen airport (ENGM)**, we consider the following waypoints of the North-Western to South-Eastern PM systems: *GM429*, *GM432*, *GM418*, *GM423*, *GM405*, *GM410*, *GM416*, and *GM411*, marked with red circles. Figure 5 - e illustrates the results of the PM catchment algorithm for the North-Western PM system.

South Korean **Incheon airport (RKSI)** implemented Eastern and Western parts of the PM systems. In this work, we investigate only the Eastern part, as for the other one the utilization of the Western part is negligibly low. The first waypoints of the sequencing legs assigned the catchment areas are *NODUN* and *UPSOM* (marked with red circle in Figure 5 - f). We consider also *ANYANG* (marked with blue circle), to filter out arrival flights which pass *NODUN* or *UPSOM* but then turn directly towards the runway missing the merge point of the PM system.

**Colombian airport (SKBO)** operates one PM system with overlapping sequencing legs. To identify the flights performing the PM procedures, we allocate catchment area circles around *PAPET* and *IRUPU* waypoints (marked with red circles in Figure 5 - g). We also add a catchment area around



, f) Seoul-Incheon (December), g) Bogotá El Dorado (second week of December), h) St. Petersburg-Pulkovo South-East (August).

**Figure 5.** Point Merge flights captured by the catchment algorithm for: a) London-City (June), b) Dublin East (second week of July), C) Dublin West (fourth week of July), d) Bergen North-West (October), e) Oslo-Gardermoen North-West (October)

the *NOR02* waypoint (marked with blue circle) to capture the inbound traffic joining the PM systems from North-West.

For the two PM systems at **St. Petersburg airport (ULLI)** we use the waypoints *LI739*, *LI760*, *LI725*, and *LI748* (marked with red circles in Figure 5 - h showing the western PM system), for NW, NE, SW, and SE PM parts, respectively.

#### 4.0.2 Step 2: Vertical Check

In the second step of the algorithm, the vertical profiles of the trajectories are considered. PM systems implement specific flight levels for the sequencing leg arcs or at least for the first waypoint on the

sequencing legs. We examine the vertical profiles of flights identified as adhering to PM in the previous step and investigate their flight levels. The required flight levels corresponding to the PM procedures of the airports in this study are as follows:

- **London City airport (EGLC)** - FL100 for the inner sequencing leg and FL090 for the outer sequencing leg
- **Dublin airport (EIDW)**
  - Western PM - FL080 for the Northern sequencing leg and FL070 on the Southern one
  - Eastern PM - FL080 for the inner sequencing leg and FL070 for the outer one
- **Bergen airport (ENBR)** - lower boundary for all PM systems is 4000 feet and upper boundary is 8000 feet
- **Oslo Gardermoen airport (ENGM)** - strict requirement to enter the PM sequencing legs at FL90, FL100, or FL110, depending on which direction the aircraft arrives from, and then with option to descend until 5000 feet with exception in North-Eastern PM where the descend can be until 6000 feet
- **Seoul Incheon airport (RKSI)** - lower boundary FL180 with option to descend until FL160 when performing holding procedure
- **Bogotá El Dorado airport (SKBO)** - strict requirement 18000 feet for inner sequencing leg and 17000 feet for the outer one
- **St. Petersburg Pulkovo airport (ULLI)** - upper boundary of FL060 for the inner sequencing leg and FL050 upper boundary for the outer one at both PM systems.

The required flight levels are specified in the respective AIP charts. We estimate the time aircraft spent on the corresponding levels, allowing for a buffer of 300 feet to account for the inaccuracies in data and control. To decide whether the aircraft spent enough time on the required flight level, we first calculate how many seconds the aircraft spent within the required flight level with the buffer, and round the result to the nearest 10. Then, we observe which time period (the values rounded to 10) is the most common among all aircraft and choose that as the decision lower boundary (threshold), for further identification on whether the flights were staying on the required level or not.

An example of vertical check part of the algorithm for the flights to Oslo Gardermoen airport is shown in Figure 6. The top two figures (Figure 6 a-b) correspond to the flights (trajectories and vertical profiles) of the Step 1 of the catchment algorithm: the flights identified as PM based on the horizontal trajectories at Step 1 and their vertical profiles, the two bottom pictures (Figure 6 c-d) represent the trajectories and vertical profiles of the PM flights after the completion of the Step 2 of the catchment algorithm, their horizontal and vertical profiles. We highlighted one example flight trajectory and its corresponding vertical profile in the pictures with clear level flight around FL100. When we compare the two trajectory pictures (Figure 6 a and c), we can clearly observe that some of the flights which were falsely identified as PM in Step 1 are filtered out in Step 2.

Vertical check enhances the horizontal part of the catchment algorithm, helping to filter out the flights identified as PM by the horizontal track, but violating the vertical requirements of the PM systems.

#### 4.0.3 Correctness Check

First, we check the correctness of the proposed catchment algorithm by visual observation. For that, we plot the horizontal tracks of the non-PM trajectories (the ones which are left in the full dataset after we remove the PM flights) together with the procedures for the corresponding airport, and check how many flights performing the PM were not identified as such. Following the visual ob-

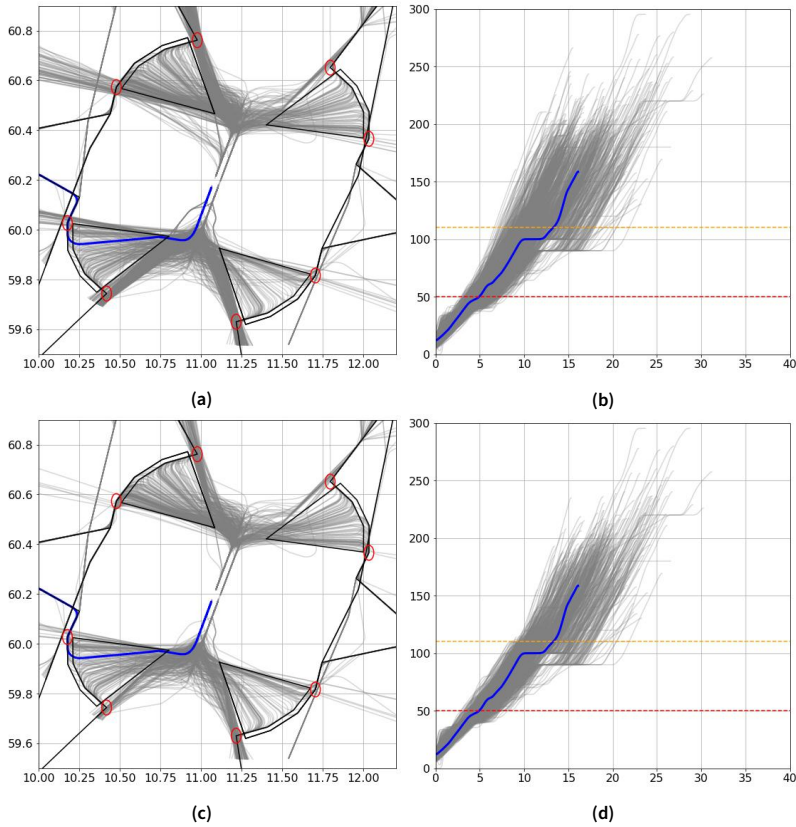


**Figure 6.** Example of the Step 2 of the catchment algorithm, the vertical check for Oslo Gardermoen airport with catchment area radius size of 0.03 DD (1.8 NM): a) The trajectories of PM identified flights after Step 1 of the algorithm (horizontal check), b) flight levels of those, c) trajectories of PM identified flights after Step 2 (vertical check), d) their flight levels.

servation and identification of false-positive or false-negative candidates, we focus on each of these candidates separately. We manually check their vertical and horizontal profiles to decide whether they were identified falsely or not. Figure 7 illustrates several examples of the non-PM figures used for the correctness check.

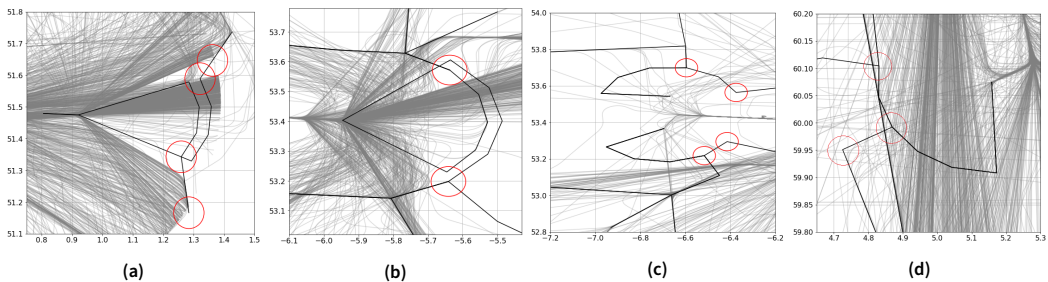


**Figure 7.** Example of the correctness check for: a) London-City (June), b) Dublin Eastern PM (second week of July), c) Dublin Western PM (fourth week of July), d) Bergen South-Western PM (October).

## False Positives

Next, we evaluate the correctness of the algorithm by calculating the number of false-positive flights,

the ones which were identified as PM flights by the catchment algorithm, but in fact did not perform the PM procedures. False-positive flights are often the ones which fly directly to the merge point without contributing to the traffic on the arcs but close enough the catchment areas to be included into the PM datasets. Table 3 presents the number of such flights for all the airports in our study, the false-positive (FP) flight numbers are in the fourth and fifth columns. The last column *False-positive flights percent* represents the percentage of the false-positive flights from all flights caught by the PM catchment algorithm.

### False Negatives

False-negative flights are those which were filtered-out as non-PM at Step 1 of the catchment algorithm. To illustrate the problem, we give an example of the false-negative flight identified by our algorithm as non-PM at Bogotá El Dorado airport (SKBO). All non-PM flights filtered out after Step 1 of the algorithm are shown in gray in Figure 8 for both directions of the PM arcs. We show horizontal and vertical profiles of the example false-negative flight in question, highlighted with blue color. The flight was not caught by the catchment algorithm at Step 1 because it started outside of the predefined procedures (black lines). The flight was added to the PM dataset after Step 2 of the algorithm, as its vertical profile corresponds to the PM level requirement. Similar inconsistencies were observed in the other data subsets as well the last two rows in Table 3 shows the amounts of false-negative (FN) flights discovered.

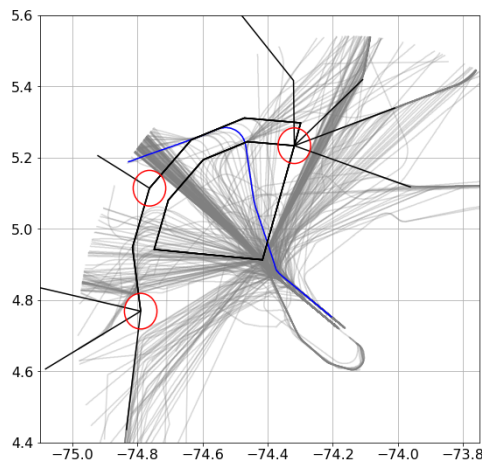


**Figure 8.** Example of false negative flights arriving at Bogotá El Dorado airport during the fourth week of December 2023.

**Table 3.** Number of PM, false-positive flights classified as PM by the catchment algorithm, and the false-negative flights

Airport ICAO	Number of all flights	Number of PM flights	Number of FP	% FP	Number of FN	% FN
EGLC	2030	163	2	1.2%	3	1.8%
EIDW	8648	3623	108	2.9%	58	1.6%
ENBR	3464	323	71	18%	11	3.3%
ENGM	7788	883	15	1.7%	8	0.9%
RKSI	1419	96	16	14.3%	0	0%
SKBO	8989	3530	262	6.9%	154	4.2%
ULLI	6462	1020	39	3.7%	13	0.7%

4.0.4 Sensitivity Analysis

To minimize the false-positive and false-negative occurrences, we tested the sensitivity of our algorithm to the size of the catchment area circle radius in Step 1. The default size of the radius is 0.05 decimal degree (DD) which is approximately 3 NM. We variate the radius sizes between 0.03 and 0.015 with the step of 0.005 decimal degrees. For the special case (SKBO) where the default radius size is too small, we tested larger values between 0.05 and 0.07 with 0.005 decimal degree step.

To decide for the best size of the catchment area radius, we variate the size and calculate the corresponding number of flights identified as PM, checking for false-positive and false-negative flight among the resulting trajectories. The goal is to choose the radius size with the minimum number of outliers (false-positives and false-negatives). The resulting numbers of PM flights are presented in Table 4, where the ones for the best chosen radius sizes for each airport are highlighted with red. Table 5 illustrates the decision process. We analyze whether the false-positive or false-negative flights were detected for various radii of the catchment area, and then choose the radius with the minimum number of outliers for each airport and PM system.

Table 4. Sensitivity Analysis: The number of PM flights based on the circle radius

Airport ICAO	Radius sizes in DD					
	0.05	0.03	0.025	0.02	0.015	
	The number of identified PM flights					
EGLC	476	296	251	199	144	
EIDW (East)	3603	3467	3333	3163	2870	
EIDW (West)	1090	955	905	841	787	
ENBR	556	401	353	218	198	
ENGM	1900	1355	1158	978	737	
RKSI	137	128	124	115	103	
ULLI	1960	1483	1243	1015	954	
	0.07	0.065	0.06	0.055	0.05	0.03
SKBO	6819	6627	6447	6292	6051	4835

Table 5. Sensitivity Analysis: false-negative and false-positive flights for various catchment area sizes

Airport ICAO	Radius sizes in DD											
	0.05	0.03	0.025	0.02	0.015		0.05	0.03	0.025	0.02	0.015	
	Detected false-negative flights?						Detected false-positive flights?					
EGLC	Yes	Yes	Yes	Yes	Yes		Yes	Yes	No	No	No	
EIDW (East)	Yes	Yes	Yes	Yes	Yes		Yes	No	No	No	No	
EIDW (West)	No	No	No	Yes	Yes		Yes	Yes	Yes	No	No	
ENBR	No	No	No	Yes	Yes		Yes	Yes	No	No	No	
ENGM	No	No	Yes	Yes	Yes		Yes	No	No	No	No	
RKSI	No	No	Yes	Yes	Yes		No	No	No	No	No	
ULLI	No	Yes	Yes	Yes	Yes		Yes	Yes	No	No	No	
	0.07	0.065	0.06	0.055	0.05	0.03	0.07	0.065	0.06	0.055	0.05	0.03
SKBO	Yes	Yes	Yes	Yes	Yes	Yes	Yes	Yes	No	No	No	No

Additionally, we inspected the relative sizes of airports and single PM systems with the goal to test the dependencies between the airport/PM system size and the size of the selected catchment area radius. Table 6 summarizes the results. All the values are taken from the corresponding AIP charts,

the lengths of the outer sequencing legs are considered for the PM Length values, and in case of inconsistent spacing between the waypoints along the sequencing legs, the most frequent value is used for the *Arcs Spacing* column. For the Airport Width and Airport Length, the peripheral points of the corresponding TMAs are used (they define the perimeter around the airport, covering the TMAs).

**Table 6.** Airport and PM system sizes

Airport ICAO	PM Length	Arcs Spacing	Airport Width	Airport Length	Rectangle
EGLC	16.2 NM	5 NM	198.6 km	170.9 km	33941 km <sup>2</sup>
EIDW (East)	28 NM	7 NM	124.6 km	203.3 km	25331 km <sup>2</sup>
EIDW (West)	30 NM	6 NM			
ENBR	18 NM	3.5 NM	103.3 km	155 km	16011 km <sup>2</sup>
ENGM	18.2 NM	6.6 NM	156.7 km	174.8 km	27391 km <sup>2</sup>
RKSI	19.2 NM	9.6 NM	207.3 km	142.6 km	29561 km <sup>2</sup>
SKBO	53.2 NM	10.4 NM	240.7 km	195.8 km	47129 km <sup>2</sup>
ULLI (East)	41 NM	9 NM	201.5 km	148.9 km	30003 km <sup>2</sup>
ULLI (West)	43 NM	9 NM			
Correlation with the chosen radius size	0.46	0.45	0.29	0.52	0.59

We examined the correlation between the chosen airport and PM size metrics and the values of the best radius sizes for the catchment areas. Unfortunately, no significant correlation was discovered. The highest correlation coefficient, but still non-significant (0.59), was observed for the correlation between the chosen radius sizes and the size of the airport perimeter (the axis-aligned geographical bounding box around the TMA) for the airports. We conclude that the size of the catchment area radius still needs to be chosen manually on experimental basis.

#### 4.1 Comparison to the Traffic Library

Traffic library [18] is a useful tool for commonly applied techniques, which also provides an easy access to the Opensky Database [29]. The tool is implemented using Python programming language. Besides many other applications, the Traffic library contains a function to identify flight trajectories adhering to the PM procedures in any set of trajectory data. The function inputs the merge point of the given PM system described in the Navaid database [30], and checks for the trajectories following a circle around the given Merge Point at a certain distance based on the AIP charts.

We use this application of the Traffic library to calculate the number of PM-adherent flights for the same seven airports in this study, for the same time periods which we've chosen our datasets for, and then compare the results of the two approaches. (Disclaimer: We encountered a problem with the data obtained using the Traffic library for Oslo Gardermoen airport. As a result, the dataset for ENGM obtained through the traffic library is incomplete. However, the error was found in a single parquet containing the flights for one day, specifically the 24<sup>th</sup> of October 2022. As a result, the final dataset used for this comparison covers 30 days instead of 31.)

The results of this comparison are shown in Table 7. The values in the table are given in the number of flights. The catchment algorithm column contains the number of flights detected by our enhanced two-step catchment algorithm with vertical profiles of flight trajectories taken into account. The Traffic library column lists the number of PM-adherent flights detected by the traffic library algorithm. The column Difference provides information about the difference in the numbers from the two preceding columns, while the last column presents the one calculated in percent. Example PM flights identified by the two algorithms in Oslo Gardermoen and Bergen airports are shown in

**Table 7.** Number of PM Flights Identified by Our Catchment Algorithm and the Traffic Library

Airport	Month	Catchment algorithm	Traffic library	Difference	Difference in percent
EGLC	June	163	162	-1	-0.6%
EIDW (East)	July	3144	3047	-97	-3%
EIDW (West)	July	479	10	-469	-98%
ENBR	October	323	135	-188	-58%
ENGM	October	883	560	-323	-37%
RKSI	December	96	24	-72	-75%
ULLI	August	1020	2226	+1206	118%
SKBO	December	3530	2912	-618	-18%

Figure 9.

The comparison results can be systematized using the following approach. As indicated in Section 3.1, the seven airports have different Point Merge system configurations. London City airport, Eastern PM at Dublin airport, Oslo Gardermoen airport, South Korean Seoul Incheon airport, St. Petersburg Pulkovo airport, and Bogotá El Dorado airport all feature the fully overlapping types of PM systems. Bergen and Eastern PM of the Dublin airport are the only examples of fully separated PM systems. With the exception of Oslo Gardermoen airport (difference of 37%), St. Petersburg Pulkovo airport (difference of 118%), and Seoul Incheon airport (difference of 75%), for which the difference between the approaches is quite significant, all the other airports with overlapping PM systems show similar values of number of PM flights (below 20%) which leads to a conclusion that despite the differences in the two algorithms, they both catch approximately the same number of flights for the airports with fully overlapping PM sequencing legs.

Within this study, we did not have the opportunity to investigate the methodology implemented in the traffic library algorithm and compare it to our catchment algorithm, but we believe that such investigation would bring interesting findings. Similarly, we can not draw conclusions on which of the algorithms has higher accuracy as there is no ground truth available at the moment. Furthermore, the future work could focus on the detailed comparison of the actual flight trajectories which were identified as PM by one algorithm and left out by the other.

## 5. PM Usage and Utilization

In this section, we present the results of evaluation using the PM usage and PM utilization metrics at the seven airports chosen for this study.

### 5.1 PM Usage

We evaluate the PM usage for each airport and present the results in Table 8. The Table 8 shows both, the results from the initial calculations (with the fixed catchment radius size of 3 NM and only horizontal check) and the calculations for the data from the enhanced catchment algorithm (adapted catchment radius size and two-step algorithm), for comparison. We conclude that in the initial calculations, the PM systems are used by about 34% of the flights in average over the airports in the study, with the maximum observed at Bogotá El Dorado (67%), and the next highest in Dublin (51%). The PM systems are not used that often in Seoul Incheon airport (9%) and Bergen airport (16%).

When using the enhanced catchment algorithm, the PM usage is significantly lower as the average value among all the airports is about 19% which is a little bit over half of the initial average value

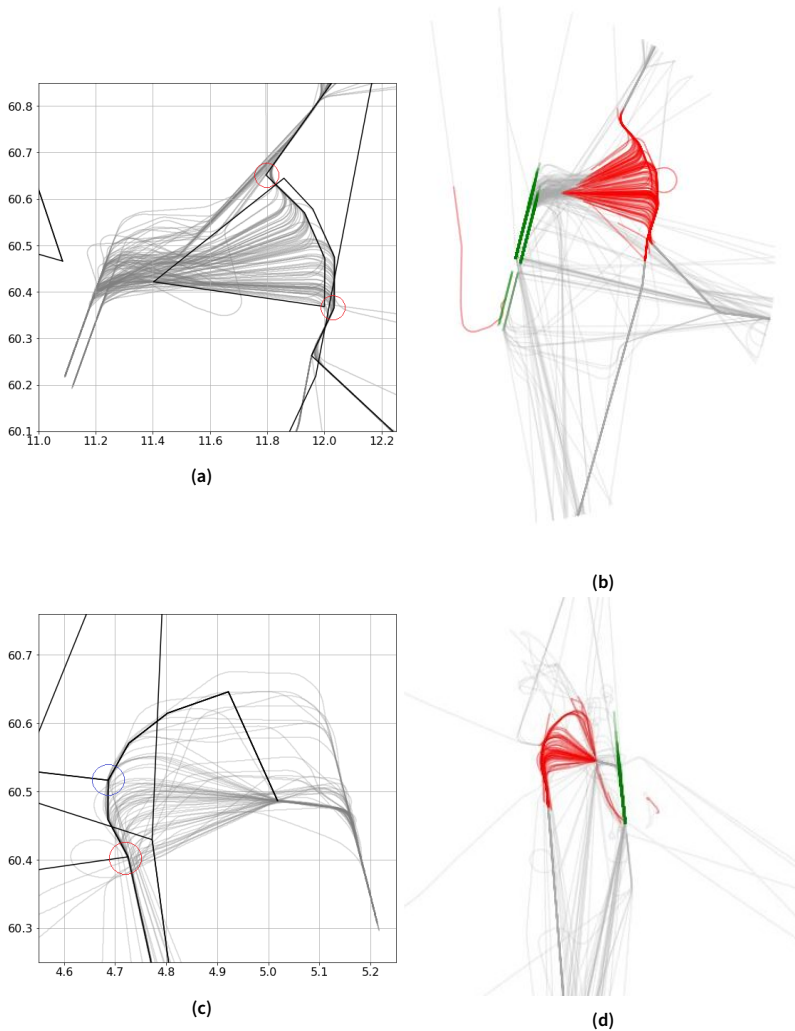


**Figure 9.** Examples of the PM flights identified by our catchment algorithm and the Traffic library algorithm for Oslo Gardermoen and Bergen airports: a) PM flights identified by our catchment algorithm from NE direction at Oslo Gardermoen airport, b) PM flights from NE direction identified by the Traffic library, c) PM flights identified by our catchment algorithm for the NW PM system of Bergen airport, d) PM flights identified by the Traffic library for the NW PM of Bergen airport.

of PM usage. Similar trend can be observed for each of the airports separately except the Dublin airport. The PM usage for Dublin airport decreased from the initial 51% to 42% which might indicate that the initial catchment algorithm was almost good enough for the Dublin airport’s PM system.

Additionally, we discovered that most of the airports do not use the PM sequencing legs evenly, some sequencing legs are used with higher frequency. In Table 9 we summarize the percentage of usage of the different sequencing legs from the PM datasets for each airport with the initial catchment area radius size of 3 NM.

### 5.2 PM Utilization

We present the results obtained for PM utilization in Tables 10, 11, 12, 13, 14, 15, 16 for EGLC, EIDW, ENBR, ENGM, RKSI, SKBO and ULLI airports, respectively. EIDW, RKSI, and SKBO airports tables contain two different subtables with the results which is caused by the fact that the PM systems at these airports are not unified and each PM system, or even each sequencing leg of one PM system (EIDW and SKBO), operates with different number of waypoints along the sequencing leg. And since we apply the catchment areas around the waypoints, the way how the sequencing legs are partitioned differ between the PMs. We include a summarizing row *All PM*, to the tables where it is suitable, which gives information about the overall PM Utilization performance of that airport. In the ‘all PM’ row, the PM Utilization values are calculated based on the accumulated values from each of the contributing sequencing legs. The calculations are based on all the trajectories passing each segment regardless of the sequencing leg location, and then we calculate the corresponding percentage from that.

We conclude that most of the airports do not utilize the full capacity of their Point Merge systems, i.e. rarely use the whole length of the sequencing legs to provide the aircraft separation and sequencing. These findings suggest, that the current procedures at the airports are designed with the spare capacity to accommodate the predicted increase in air traffic in the future. Another reason for implementing PM is to improve vertical efficiency. Further investigations would be needed in order to determine whether the current designs satisfy the needs of each particular airport. ULLI has the highest proportion of the flights which reached to the final turning point of the corresponding sequencing leg. RKSI and ENGM are the airports with the highest proportion of the flights which turn towards the Merge Point directly after entering the PM systems.

The comparative results for the PM Utilization at different airports are illustrated in Figure 10 with a cumulative function showing the percentage of flights utilizing up to a certain percent/portion of the

**Table 8.** PM Usage Calculated For the Initial One-Step Algorithm (with radius of 3 NM) and for the Enhanced Two-Step Algorithm (with the adapted radius size)

Airport ICAO	# PM flights	# all flights	PM usage	# PM flights (new algorithm)	PM Usage (new algorithm)
EGLC	476	2030	23.6%	163	8%
EIDW	4685	8648	51.2%	3623	41.9%
ENBR	556	3464	16.1%	323	9.3%
ENGM	1900	7788	24.4%	883	11.3%
RKSI	137	1419	9.65%	96	6.8%
SKBO	6051	8989	67.3%	3530	39.3%
ULLI	1960	6462	30.3%	1020	15.8%

**Table 9.** PM Usage for Different Sequencing Legs (in % of PM Flights)

Airport	Leg 1	Leg 2	Leg 3	Leg 4	Leg 5	Leg 6	Leg 7	Leg 8
EGLC	North (80%)	South (20%)						
EIDW	NW (12%)	SW (8%)	NE(38%)	SE (42%)				
ENBR	NW (69%)	SW (2%)	NE (22%)	SE (7%)				
ENGM	NW1 (27%)	NW2 (8%)	SW1 (8%)	SW2 (24%)	NE1 (5%)	NE2 (4%)	SE1 (3%)	SE2 (21%)
RKSI	North (0%)	South (100%)						
SKBO	West (70%)	East (30%)						
ULLI	NW (38%)	SW (30%)	NE (17%)	SE (15%)				

**Table 10.** PM Utilization EGLC

Original Radius 0.05 (3 NM)					
Airport ICAO	PM system	Only start	One-third	Two-thirds	Full arc
EGLC	North	76.3%	14.2%	6.4%	3.2%
EGLC	South	61.5%	25%	9.4%	4.2%
EGLC	All PM	73.3%	16.4%	6.9%	3.4%
Revised Radius 0.025 (1.5 NM)					
Airport ICAO	PM system	Only start	One-third	Two-thirds	Full arc
EGLC	North	51.5%	30.3%	10.1%	8.1%
EGLC	South	60.3%	30.2%	7.9%	1.6%
EGLC	All PM	54.9%	30.3%	9.3%	5.6%

**Table 11.** PM Utilization EIDW

Original Radius 0.05 (3 NM)							
Airport ICAO	PM system	Only start	One-quarter	Half	Three-quarters	Full arc	
EIDW	South-West	38.6%	28.2%	14%	15.4%	3.9%	
EIDW	East	57.4%	18.9%	13.8%	7.7%	2.3%	
EIDW	SW and E	55.8%	19.7%	13.8%	8.3%	2.5%	
Airport ICAO	PM system	Only start	20%	40%	60%	80%	Full arc
EIDW	North-West	34.9%	44%	7.7%	5.6%	6.2%	1.8%
Revised Radius 0.02 (1.2 NM) for West and 0.05 (3 NM) for East							
Airport ICAO	PM system	Only start	One-quarter	Half	Three-quarters	Full arc	
EIDW	South-West	38.2%	22.4%	16.2%	22.8%	0.4%	
EIDW	East	50%	22%	16.2%	9.1%	2.8%	
EIDW	SW and E	49.2%	22%	16.2%	10%	2.6%	
Airport ICAO	PM system	Only start	20%	40%	60%	80%	Full arc
EIDW	North-West	51%	13.2%	11.2%	13.2%	9.2%	2%

PM arc. The utilization curves for all airports follow similar shape, i.e. very steep descent until approximately 30% of the PM arcs length, with very small utilization values for the rest. Except Bergen airport, most flights leave the PM arcs before they reach 50% of their lengths. Bergen airport and the western PM system of Dublin airport both operate with dissociated sequencing legs, however, no clear connection in between PM utilization of these two PM systems can be seen in Figure 10. We also observe similar shape of the PM utilization curves for Oslo Gardermoen airport with the adjusted radius size and for London city airport, despite the fact that they both use PM system with fully overlapping sequencing legs, we don't have a clear explanation for such similarity as ENGM operates four PM systems and EGLC only one.

Additionally, we provide pie charts in Figure 11 illustrates the PM usage for each airport to improve the readability of the results. The pie charts visualize the whole flight arrival datasets, where the blue parts represent all the arrival trajectories filtered out as non-PM flights, and the orange and green wedges together represent all the flight trajectories identified as PM flights. The green wedges correspond to the proportion of the PM flights which enter the PM system but touching only the first waypoint of the sequencing leg and turning directly to the merge point. Similarities can be observed for EIDW and SKBO airports, featuring significant amount of PM flights, which can be explained by the fact that they both accommodate high density traffic.

**Table 12. PM Utilization ENBR**

Original Radius 0.05 (3 NM)							
Airport ICAO	PM system	Only start	20%	40%	60%	80%	Full arc
ENBR	North-West	22%	23%	45.5%	5.2%	1.3%	3.1%
ENBR	North-East	16.1%	24.2%	25.8%	14.5%	9.7%	9.7%
ENBR	South-West	55.6%	22.2%	22.2%	0%	0%	0%
ENBR	South-East	68.3%	9.8%	12.2%	2.4%	7.3%	0%
ENBR	All PM	24.6%	22.3%	38.3%	7%	3.6%	4.3%
Revised Radius 0.025 (1.5 NM)							
Airport ICAO	PM system	Only start	20%	40%	60%	80%	Full arc
ENBR	North-West	30.1%	19.4%	30.1%	8.6%	6.5%	5.4%
ENBR	North-East	89.8%	3.2%	3.4%	2.1%	0.8%	0.8%
ENBR	South-West	97.7%	2.3%	0%	0%	0%	0%
ENBR	South-East	87.2%	5.1%	3.9%	1.3%	2.6%	0%
ENBR	All PM	82.2%	5.4%	6.5%	2.5%	1.6%	1.2%

**Table 13. PM Utilization ENGM**

Radius 0.05 (3 NM)					
Airport ICAO	PM system	Only start	One-third	Two-thirds	Full arc
ENGM	North-West	72.1%	13.8%	1.8%	12.3%
ENGM	North-East	69.7%	26.9%	2.3%	1.1%
ENGM	South-West	88.7%	8.7%	1.8%	0.8%
ENGM	South-East	90.3%	5.4%	1.6%	2.7%
ENGM	All PM	81.4%	11.4%	1.8%	5.4%
Radius 0.03 (1.8 NM)					
Airport ICAO	PM system	Only start	One-third	Two-thirds	Full arc
ENGM	North-West	76.1%	19.2%	2.9%	1.8%
ENGM	North-East	67.2%	28.6%	4.2%	0%
ENGM	South-West	77%	18%	4.5%	0.5%
ENGM	South-East	87.4%	6.6%	3%	3%
ENGM	All PM	77.8%	17.2%	3.6%	1.5%

**Table 14. PM Utilization RKSI**

Original Radius 0.05 (3 NM)				
Airport ICAO	PM system	Only start	Half	Full arc
RKSI	North	0%	0%	0%
RKSI	South	96.4%	2.9%	0.7%
Revised Radius 0.03 (1.8 NM)				
Airport ICAO	PM system	Only start	Half	Full arc
RKSI	North	0%	0%	0%
RKSI	South	83.4%	3.1%	12.5%

**Table 15.** PM Utilization SKBO

Original Radius 0.05 (3 NM)							
Airport ICAO	PM system	Only start	One-quarter	Half	Three-quarters	Full arc	
SKBO	East	43.1%	33.4%	15.1%	6%	2.4%	
Airport ICAO	PM system	Only start	20%	40%	60%	80%	Full arc
SKBO	West	46.8%	24.8%	12.3%	4.5%	2.4%	9.3%
Revised Radius 0.06 (3.6 NM)							
Airport ICAO	PM system	Only start	One-quarter	Half	Three-quarters	Full arc	
SKBO	East	45.1%	31.9%	15.2%	5.6%	2.2%	
Airport ICAO	PM system	Only start	20%	40%	60%	80%	Full arc
SKBO	West	31.5%	13.7%	38.6%	8.2%	2.1%	5.9%

**Table 16.** PM Utilization ULLI

Original Radius 0.05 (3 NM)						
Airport ICAO	PM system	Only start	One-quarter	Half	Three-quarters	Full arc
ULLI	North-West	74.4%	9.2%	7%	4.6%	4.7%
ULLI	North-East	51.1%	16.7%	14.3%	6%	11.9%
ULLI	South-West	31.8%	24.3%	15.6%	11.4%	16.9%
ULLI	South-East	0%	39.6%	30.9%	18.1%	11.4%
ULLI	All PM	54.2%	16.5%	12%	7.5%	9.7%
Revised Radius 0.025 (1.5 NM)						
Airport ICAO	PM system	Only start	One-quarter	Half	Three-quarters	Full arc
ULLI	North-West	55.2%	14.7%	13.4%	12.4%	4.3%
ULLI	North-East	46.8%	26.6%	11.4%	13.3%	1.9%
ULLI	South-West	6.1%	30.9%	24.6%	30.6%	7.9%
ULLI	South-East	0%	42.6%	34.8%	20.9%	1.7%
ULLI	All PM	37.5%	23%	17.4%	17.8%	4.3%

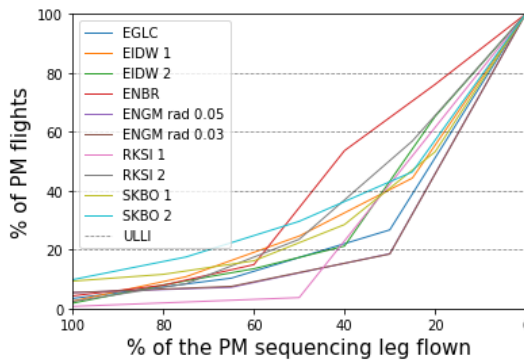


**Figure 10.** Cumulative PM utilization of the seven airports in the study.

## 6. Conclusions and Future Work

In this work, we investigated the PM arrival procedures implemented at seven airports around the globe. We proposed a two-step catchment algorithm to create datasets containing the flights adher-

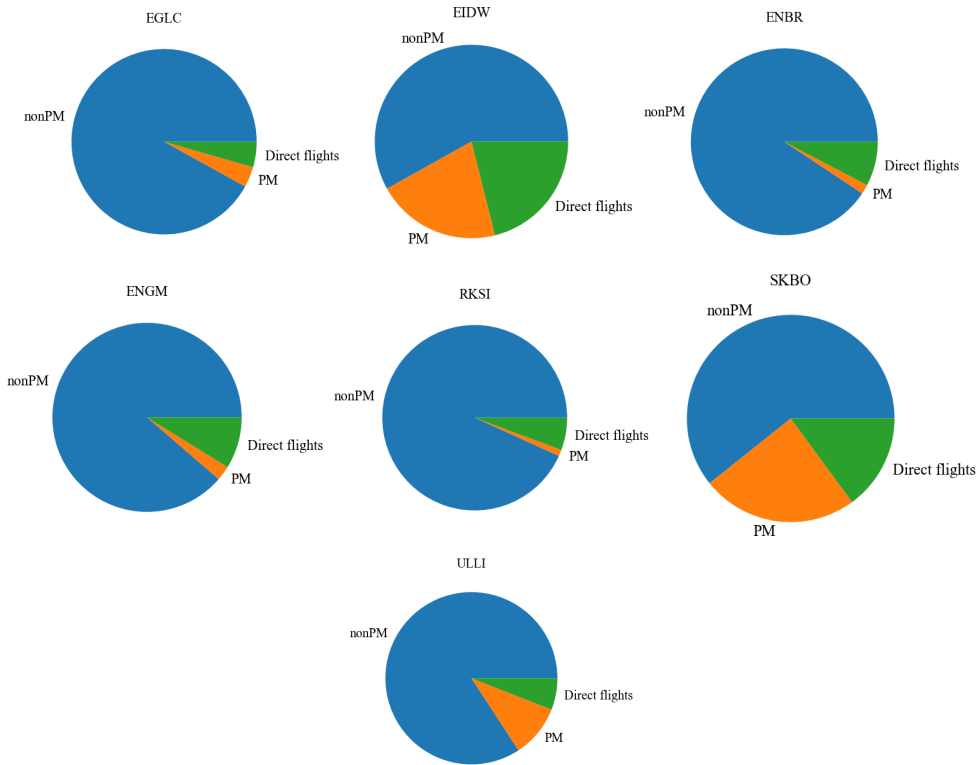


Figure 11. Pie chart visualization of PM usage for each airport.

ent to the PM arrival procedures for further analysis. We justified the correctness of our algorithm analysing the flights identified as non-PM, and confirmed that most of the flights were attributed correctly with minor exceptions. After previous sensitivity test of the algorithm to the changes in the radius of the catchment area circle, we utilized the flexible (best for each airport) circle size of the catchment algorithm. We enriched the algorithm by considering the vertical profiles of the flights according to the required published PM flight levels.

Using the PM datasets for each airport, we calculated the PM usage and PM utilization metrics which were developed specifically for evaluation of the Point Merge procedures. The PM usage largely varies with the average value of 19%. The PM Utilization results indicate that the capacity of the PM sequencing legs is underutilized at most of the airports in our studies, which uncovers that the PM systems have a potential to accommodate higher traffic volumes in the future. When the PM sequencing legs are utilized to the full extent frequently, it may be a sign that the arrival capacity of the systems is not sufficient. This study reports the current state of usage of the implemented Point Merge systems on various airports and we believe it can be a tool for the ATCs to evaluate whether the implemented PM system serves the purpose of the design.

In future work, we consider more detailed performance analysis based on the obtained PM datasets, targeting better understanding of the trade-offs associated with different design options of the PM systems, and aiming optimization of the PM usage.

## Author contributions

- Tatiana Polishchuk: Conceptualization, Methodology, Investigation, Paper Writing
- Lucie Smetanová: Data curation, Methodology, Implementation, Investigation, Paper Writing
- Henrik Hardell: Methodology, Investigation, Data curation

Note, that in this paper the author names are listed in the alphabetical order.

## Funding statement

This research is supported by the Swedish Transport Administration (Trafikverket) and in-kind participation of LFV within the ODESTA-PM and TMAKPI projects.

## Open data statement

The authors completely support the open access data initiative. The datasets created for these studies are provided in [https://github.com/LucieSmetanova/JOAS\\_Journal\\_Paper\\_2204](https://github.com/LucieSmetanova/JOAS_Journal_Paper_2204). The provided repository contains source codes, datasets and instructions how to use them.

## Reproducibility statement

Information on how to reproduce this research, including access to 1) source code related the research, 2) source code for the figures is provided in [https://github.com/LucieSmetanova/JOAS\\_Journal\\_Paper\\_2204](https://github.com/LucieSmetanova/JOAS_Journal_Paper_2204).

## References

- [1] EUROCONTROL. *Guidance Material for the Design of Terminal Procedures for Area Navigation (DME/DME, B-GNSS, Baro-VNAV & RNP-RNAV)*. EUROCONTROL, 2003.
- [2] L. Boursier, B. Favennec, E. Hoffman, A. Trzmiel, F. Vergne, and K. Zeghal. “Merging arrival flows without heading instructions”. In: *7th USA/Europe air traffic management R&D seminar*. 2007, pp. 1–8.
- [3] B. Favennec, T. Symmans, D. Houlihan, K. Vergne, and K. Zeghal. *Point Merge Integration of Arrival Flows Enabling Extensive RNAV Application and Continuous Descent–Operational Services and Environment Definition*. OSED. 2010.
- [4] International Civil Aviation Organization. *Air Traffic Management: Procedures for Air Navigation Services, Doc 4444 ATM/501*. 2007.
- [5] Ö. S. Meric and O. Usanmaz. “A new standard instrument arrival: the point merge system”. In: *Aircraft Engineering and Aerospace Technology* (2013).
- [6] D. Ivanescu, C. Shaw, C. Tamvaclis, and T. Kettunen. “Models of air traffic merging techniques: evaluating performance of point merge”. In: *9th AIAA Aviation Technology, Integration, and Operations Conference (ATIO) and Aircraft Noise and Emissions Reduction Symposium (ANERS)*. 2009, p. 7013.
- [7] M. Liang, D. Delahaye, and P. Maréchal. “Potential operational benefits of multi-layer point merge system on dense TMA operation hybrid arrival trajectory optimization applied to Beijing capital international airport”. In: *Proceedings of the 7th International Conference on Research in Air Transportation*. 2016.
- [8] Y. Hong, B. Choi, K. Lee, and Y. Kim. “Dynamic Robust Sequencing and Scheduling Under Uncertainty for the Point Merge System in Terminal Airspace”. In: *IEEE Transactions on Intelligent Transportation Systems* 19 (2018), pp. 2933–2943. URL: <https://api.semanticscholar.org/CorpusID:52195971>.

- [9] EUROCONTROL. *Point Merge Implementation: a quick guide. White paper*. <https://www.eurocontrol.int/publication/point-merge-implementation>. last accessed on 05.07.2024. 2021.
- [10] H. Hardell, T. Polishchuk, and L. Smetanová. “Investigation of Point Merge Utilization Worldwide Using Opensky Network Data”. In: *Proceedings of the 11th Opensky Symposium 2023 in the Journal of Open Aviation Science* 1.2 (2023).
- [11] B. Favennec, E. Hoffman, A. Trzmiel, F. Vergne, and K. Zeghal. “The Point Merge Arrival Flow Integration Technique: Towards More Complex Environments and Advanced Continuous Descent”. In: Sept. 2009. ISBN: 978-1-60086-977-8. DOI: 10.2514/6.2009-6921.
- [12] M. Liang, D. Delahaye, and P. Maréchal. “A framework of point merge-based autonomous system for optimizing aircraft scheduling in busy TMA”. In: *5th SESAR Innovation Days, Bologna, Italy* (2015).
- [13] Wilde J.M. *Implementing point merge system based arrival management at Amsterdam Airport Schiphol. MS thesis*. <http://repository.tudelft.nl/>. August 2018.
- [14] L. S. Rebollar. *Automation Control of a Point Merge System at Palma de Mallorca airport*. Bachelor Thesis, UPC Barcelona. 2019.
- [15] C. Raphael, B. Favennec, E.G. Hoffman, and K. Zeghal. “Detecting Point Merge patterns using computer vision”. In: *AIAA AVIATION 2021 FORUM*. 2021, p. 2390.
- [16] Thomas Schneider, Bruno Favennec, Joana Frontera-Pons, Eric Hoffman, and Karim Zeghal. “Detecting Point Merge Patterns From Track Data”. In: *2020 Integrated Communications Navigation and Surveillance Conference (ICNS)*. 2020, 5A2-1-5A2-16. DOI: 10.1109/ICNS50378.2020.9223006.
- [17] X. Olive, J. Sun, L. Basora, and E. Spinielli. “Environmental inefficiencies for arrival flights at European airports”. In: *PLOS ONE* (June 2023). DOI: 10.1371/journal.pone.0287612.
- [18] X. Olive. “Traffic: a toolbox for processing and analysing air traffic data”. In: *Journal of Open Source Software* 4.39 (2019), pp. 1518-1. DOI: 10.21105/joss.01518.
- [19] Kadir Dönmez, Cem Çetek, and Onur Kaya. “Air traffic management in parallel-point merge systems under wind uncertainties”. In: *Journal of Air Transport Management* 104 (2022), p. 102268. ISSN: 0969-6997. DOI: <https://doi.org/10.1016/j.jairtraman.2022.102268>. URL: <https://www.sciencedirect.com/science/article/pii/S0969699722000886>.
- [20] Bruno Favennec, Aymeric Trzmiel, and Karim Zeghal. *The "double" Point Merge: large capacity in a small area - Extension of an arrival sequencing technique for application to airspace-constrained terminal areas*. June 2024. DOI: 10.13140/RG.2.2.29010.77767/1.
- [21] H. Hardell, A. Lemetti, T. Polishchuk, and L. Smetanová. “Performance Characterization of Arrival Operations with Point Merge at Oslo Gardermoen Airport”. In: *15th USA/Europe Air Traffic Management Research and Development Seminar (ATM2023), Savannah, Georgia, June 5-9, 2023*. 2023.
- [22] EUROCONTROL Experimental Centre. *Point Merge: Improving and harmonising arrival operations*. URL: <https://www.eurocontrol.int/concept/point-merge>.
- [23] UK AIP. <https://nats-uk.ead-it.com/cms-nats/opencms/en/Publications/AIP/>. last accessed on 25.10.2023.
- [24] Irish AIP. [http://iaip.iaa.ie/iaip/aip\\_directory.htm](http://iaip.iaa.ie/iaip/aip_directory.htm). last accessed on 25.10.2023.
- [25] Norwegian AIP. <https://avinor.no/en/ais/aipnorway/>. last accessed on 25.10.2023.
- [26] Colombian AIP. <https://www.aerocivil.gov.co/servicios-a-la-navegacion/servicio-de-informacion-aeronautica-ais/aip>. last accessed on 25.10.2023.
- [27] South Korean AIP. <http://ais.casa.go.kr/>. last accessed on 25.10.2023.
- [28] Russian AIP. [https://www.caica.ru/ANI\\_Official/?lang=en](https://www.caica.ru/ANI_Official/?lang=en). last accessed on 25.10.2023.
- [29] Opensky Network. <https://opensky-network.org/>. last accessed on 11.02.2022.
- [30] European AIS Database, EUROCONTROL. <https://www.eurocontrol.int/service/european-ais-database>. last accessed on 15.06.2024.